The Astrophysical Journal, 904:183 (7pp), 2020 December 1 https://doi.org/10.3847/1538-4357/abbffe

Estimation of Thermal and Epithermal Neutron Fluences at the Lunar Surface from Isotopic Compositions of Rare Earth Elements

Hiroshi Hidaka[1], Yuki Mizutani[1], and Shigekazu Yoneda[2]
[1] Department of Earth and Planetary Science, Nagoya University, Nagoya 464-8601, Japan; hidaka@eps.nagoya-u.ac.jp
[2] Department of Science and Engineering, National Museum of Nature and Science, Tsukuba 305-0005, Japan
Received 2020 July 20; revised 2020 September 8; accepted 2020 October 8; published 2020 December 3

Abstract

Thermalized neutrons arising at the surface of solar planets are produced from the interaction of cosmic rays with the nucleus consisting of surficial materials. The neutron energy spectrum in the range between thermal and epithermal regions at the lunar surface was investigated based on the combination of the isotopic variations of Sm and Gd caused by the thermal neutron-capture reactions in our previous study, with those of Dy, Er, and Yb caused by the epithermal neutron-capture reactions in this study. The detailed comparison of the systematic isotopic variations among Sm, Gd, Dy, Er, and Yb helps to construct a neutron energy spectrum at the surface of the Moon. Seven kinds of lunar soils at different depths of the drill core recovered from the Apollo 15 landing site (A-15) were used in this study. Isotopic variations of $^{164}Dy/^{161}Dy$, $^{168}Er/^{167}Er$, and $^{168}Yb/^{174}Yb$ were newly found in the A-15 samples, and showed the depth dependence caused by the interaction with cosmic-ray irradiation. In particular, the combination of the isotopic shifts of $^{168}Er/^{167}Er$ and $^{150}Sm/^{149}Sm$ could be effectively used to evaluate the epithermal neutron fluences of 5.4–8.1 $\times$ 10^{17} n cm^{-2} that were more than 10 times higher than thermal neutron fluences of 0.48–0.69 $\times$ 10^{17} n cm^{-2} reestimated in this study.

Unified Astronomy Thesaurus concepts: Galactic cosmic rays (567); Lunar surface (974); Isotope shifts (2069)

1. Introduction

The surficial materials of solar planets without atmospheric layers are exposed to cosmic rays that include galactic cosmic rays (GCRs) with high energy and solar cosmic rays (SCRs) with low energy. GCRs interact with the upper few meters of the surface materials, while SCRs interact with very surficial parts at the upper few hundreds of μm of the grains. Many particles such as protons and neutrons are produced by spallation reactions on the surface of planetary materials by GCR irradiation.

The neutrons, generated by the spallation, lose their energy gradually after several cascade collisions with the surrounding atoms and are finally thermalized ($E < 0.1$ eV) after passing through fast (>MeV) and epithermal (0.1 eV $< E <$ 500 keV) energy regions in planetary materials. Isotopic variations in some elements constituting the planetary materials occur by neutron-capture reactions, because thermalized neutrons are sensitively captured by some nuclei with large thermal neutron-capture cross sections such as ^{149}Sm (4.01×10^4 barn), ^{155}Gd (6.09×10^4 barn), and ^{157}Gd (2.54×10^5 barn). The degree of thermalization of neutrons depends on the burial depth and the chemical compositions of the targeted planetary material (Lingenfelter et al. 1961). The detailed characteristics of neutrons generated in the target can be evaluated from the neutron energy spectrum, defined as neutron fluences as a function of the neutron energy. Reconstruction of the fine structure of the neutron energy spectra for individual planetary materials may provide some important information about the changes of shape, size, and chemical composition of the materials since their formation.

The availability and determination of lunar neutron energy spectra for deriving information about chemical compositions including hydrogen, which is related to the possibility of the existence of water on the Moon, were first suggested by Lingenfelter et al. (1961). Based on the model given by Lingenfelter et al. (1961), several calculations for neutron energy spectra have been developed for various kinds of planets and meteorites as well as for lunar surface materials (Lingenfelter et al. 1972; Spergel et al. 1986; Feldman et al. 1998a, 1998b, 2000; Leya et al. 2003; Leya & Masarik 2013). In addition, a number of studies have focused on the variations of stable isotopes due to cosmic-ray irradiation, such as ^{149}Sm, ^{155}Gd,^{157}Gd (Russ et al. 1971, 1972; Curtis & Wasserburg 1975; Hidaka et al. 2000, Hidaka & Yoneda 2007, Hidaka et al. 2009, 2017), and ^{113}Cd (Sands et al. 2001; Kruijer et al. 2013) and short-lived cosmogenic nuclides such as ^{10}Be, ^{26}Al, ^{36}Cl, and ^{41}Ca (Nishiizumi et al. 1984a, 1984b, 1997) in extraterrestrial materials. Depth profiles of the fluence of thermal neutrons ($E < 0.1$ eV) on the Moon were also discussed from isotopic variations, especially in lunar drill stem samples returned by the Apollo 15 mission (A-15), which are considered to be the best samples for studying the depth dependence of the interaction between planetary materials and cosmic rays (Russ et al. 1972; Nishiizumi et al. 1984a, 1984b, 1997; Hidaka et al. 2000). Albalat et al. (2015) analyzed Sm, Gd, Dy, Er, Yb, and Hf isotopic compositions of the Apollo lunar samples collected from different sites on the Moon, and suggested that the lunar neutron energy spectrum was richer in high-energy neutrons. In the case of meteorites, however, since the burial depth of a meteorite on the parent body is unclear, it is necessary to quantitatively estimate the neutron fluence in the range from low- to high-energy regions along with the depth direction in the parent body to discuss the temporal transition of the size and/or the chemical composition of a meteorite. Some of the Apollo samples can be good references for understanding neutron energy spectra through their interactions with GCR irradiation, because their depth information is well known.

Some isotopes of heavier rare earth elements (REEs) have a large resonance integral (RI) relative to the thermal neutron-capture cross section (σ_{th}), as listed in Table 1. Since ^{162}Dy,

Table 1
The Data for Thermal Neutron-capture Cross Sections (σ_{th}), Resonance Integrals (RIs), and Epithermal Neutron-capture Cross Section (σ_{epi}) of Selected Isotopes from Heavier REEs (Barns)

Isotope	σ_{th}	RI	σ_{epi}
^{149}Sm	4.01×10^4	3.38×10^3	4.77×10^2
^{155}Gd	6.09×10^4	1.54×10^3	2.57×10^2
^{157}Gd	2.53×10^5	7.59×10^2	1.19×10^2
^{162}Dy	1.94×10^2	2.75×10^3	2.99×10^2
^{163}Dy	1.23×10^2	1.49×10^3	1.96×10^2
^{164}Dy	2.65×10^3	3.42×10^2	3.56×10
^{167}Er	6.49×10^2	2.98×10^3	3.59×10^2
^{168}Yb	2.30×10^3	2.13×10^4	3.56×10^3
^{169}Tm	1.05×10^2	1.62×10^3	1.95×10^2

Note. The data of σ_{th} and RI for individual isotopes are given from the Evaluated Nuclear Data File (ENDF/B-VII.1) compiled by National Nuclear Data Center at Brookhaven National Laboratory (https://www.nndc.bnl.gov/sigma/index.jsp).

σ_{epi} is calculated from the equation of $\sigma_{epi} = \frac{RI}{\int_{E_c}^{E_{max}} \frac{dE}{E}}$ (see the text).

^{163}Dy, ^{167}Er, ^{168}Yb, and ^{169}Tm are expected to be sensitive enough to react with not only thermal neutrons but also epithermal neutrons because of their large RIs over 10^3 barns, their isotopic abundances of lunar surficial samples may have varied with the degree of thermalization of the neutrons arising in the subsurface of the Moon. In this study, Sm, Gd, Dy, Er, and Yb were selected as the key elements for the isotopic studies used to reconsider the details of the neutron energy spectrum on the lunar surface. In addition to thermal neutron information from the isotopic data of Sm and Gd, epithermal neutron information can possibly be obtained from the isotopic data of Dy, Er, and Yb. Possible discussion of the neutron energy spectrum of lunar surface would be given by the estimation of thermal and epithermal neutron fluences from the systematic isotopic data of REEs.

2. Experiments

2.1. Samples

The A-15 drill core with a length of 2.42 m was collected from the lunar surface at the A-15 landing site, and is suitable for exploring the depth dependence of the interaction between cosmic-ray and the planetary materials, because the depths of individual samples in the core are well known and the whole of the A-15 drill core had been stratigraphically undisturbed for a very long period of around 450 million years (Russ et al. 1972). The A-15 drill core is divided into six sections from 15001 (bottom) to 15006 (upper). Seven samples (15001.375, 15002.747, 15003.734, 15004.129, 15005.14 15005.79, and 15006.310) taken from individual sections were selected for this study. Detailed depth information of each sample is shown in Table 2. The A-15 drill-core samples are well documented, and have often been used to quantify the neutron-captured and the spallogenic products formed by the interaction with GCR irradiation (Russ et al. 1972; Nishiizumi et al. 1997; Hidaka et al. 2000). Sm and Gd isotopic measurements were previously performed in the same samples to determine the thermal neutron fluence (Russ et al. 1972; Hidaka et al. 2000). Here in this study, we newly report the isotopic data set of Dy, Er, and Yb of a series of the A-15 samples.

Table 2
Description of the Samples from the A-15 Drill Core

Sample	Depth from the surface	
	(cm)	(g cm^{-2})
15001.375	236	412
15002.747	199	341
15003.734	159	276
15004.129	120	208
15005.14	81	138
15005.79	65	109
15006.310	39	65

2.2. Chemical Separation

About 30 mg of each sample was completely decomposed by HF–$HClO_4$. The sample was redissolved in 1 mL of 1.7 M HCl. REE fractions were collected after removal of major elements from the sample solutions using a cation exchange resin packed column (Bio-Rad AG50WX8, 200–400 mesh, H^+ form, column volume 1.0 mL, i.d. 4.0 mm) with 5.0 mL of 1.7 M HCl and 5.5 mL of 6.0 M HCl as the eluent. Subsequently, for the mutual separation of Dy, Er, and Yb in REE fractions, an Ln-resin packed column (Eichrom Co. Ltd., particle size of 20–50 μm, column volume of 0.5 mL, i.d. 2.5 mm) was used. A detailed description of the conditions of the chemistry is given in our previous study (Mizutani et al. 2020). Each fraction collected by Ln-resin chemistry was evaporated to dryness, and the residue was decomposed by 0.1–0.2 mL of aqua regia.

2.3. Mass Spectrometric Analyses

A thermal ionization mass spectrometer (Triton Plus) equipped with nine Faraday cup collectors was used for the isotopic measurements of Dy, Er, and Yb. Cup configurations and the analytical conditions for individual isotopic measurements are shown in our previous study (Mizutani et al. 2020). All analyses were performed in static mode with the amplifier rotation system. $^{160}Dy/^{161}Dy = 0.123384$, $^{170}Er/^{166}Er = 0.44547$, and $^{172}Yb/^{174}Yb = 0.68321$ were used as normalizing factors of the Dy, Er, and Yb isotopic data sets, respectively, to make corrections for the instrumental isotopic mass fractionation according to the exponential law (Mizutani et al. 2020).

2.4. Epithermal Neutron-capture Cross Section

In this study, the cross sections for epithermal neutron capture are estimated from the values of RI and the integration range of the neutron adsorption resonance for individual isotopes.

In general, the RI is defined as $RI = \int_{E_c}^{E_{max}} \sigma(E) \frac{dE}{E}$ where E_c is a cutoff energy, typically used as 0.5 eV, E_{max} is the highest

Table 3
(a) Dy, (b) Er, and (c) Yb Isotopic Data

(a) Dy Isotopic Data Normalized to $^{160}Dy/^{161}Dy = 0.123384$

	$^{156}Dy/^{161}Dy$	$^{158}Dy/^{161}Dy$	$^{162}Dy/^{161}Dy$	$^{163}Dy/^{161}Dy$	$^{164}Dy/^{161}Dy$
15001	0.002862 ± 1	0.004986 ± 1	1.347585 ± 13	1.315475 ± 24	1.491662 ± 41
15002	0.002858 ± 2	0.004985 ± 1	1.347577 ± 8	1.315487 ± 14	1.491538 ± 23
15003	0.002860 ± 2	0.004982 ± 1	1.347569 ± 17	1.315481 ± 27	1.491523 ± 45
15004	0.002863 ± 3	0.004985 ± 2	1.347552 ± 19	1.315481 ± 37	1.491363 ± 41
15005.14	0.002862 ± 2	0.004986 ± 2	1.347559 ± 22	1.315482 ± 47	1.491410 ± 55
15005.79	0.002859 ± 2	0.004986 ± 1	1.347581 ± 21	1.315486 ± 34	1.491493 ± 51
15006	0.002861 ± 2	0.004982 ± 2	1.347592 ± 27	1.315482 ± 57	1.491679 ± 72
STD	0.002861 ± 2	0.004984 ± 1	1.347588 ± 14	1.315469 ± 26	1.491852 ± 38

(b) Er Isotopic Data Normalized to $^{170}Er/^{166}Er = 0.44547$

	$^{162}Er/^{166}Er$	$^{164}Er/^{166}Er$	$^{167}Er/^{166}Er$	$^{168}Er/^{166}Er$
15001	0.004049 ± 4	0.047780 ± 5	0.682569 ± 12	0.805699 ± 13
15002	0.004048 ± 5	0.047786 ± 4	0.682540 ± 8	0.805716 ± 9
15003	0.004047 ± 5	0.047785 ± 4	0.682526 ± 9	0.805728 ± 11
15004	0.004047 ± 4	0.047789 ± 5	0.682504 ± 14	0.805763 ± 16
15005.14	0.004048 ± 8	0.047785 ± 7	0.682510 ± 16	0.805742 ± 19
15005.79	0.004047 ± 4	0.047783 ± 4	0.682535 ± 12	0.805758 ± 14
15006	0.004048 ± 5	0.047787 ± 6	0.682578 ± 9	0.805688 ± 12
STD	0.004047 ± 5	0.047784 ± 1	0.682736 ± 2	0.805536 ± 2

(c) Yb Isotopic Data Normalized to $^{172}Yb/^{174}Yb = 0.68321$

	$^{168}Yb/^{174}Yb$	$^{170}Yb/^{174}Yb$	$^{171}Yb/^{174}Yb$	$^{173}Yb/^{174}Yb$	$^{176}Yb/^{174}Yb$
15001	0.003951 ± 8	0.094814 ± 6	0.445935 ± 8	0.505047 ± 7	0.402237 ± 8
15002	0.003951 ± 7	0.094814 ± 6	0.445935 ± 9	0.505030 ± 7	0.402238 ± 10
15003	0.003946 ± 5	0.094815 ± 7	0.445939 ± 8	0.505051 ± 6	0.402243 ± 10
15004	0.003945 ± 3	0.094810 ± 4	0.445932 ± 5	0.505043 ± 5	0.402230 ± 6
15005.14	0.003945 ± 5	0.094813 ± 5	0.445935 ± 7	0.505034 ± 10	0.402242 ± 7
15005.79	0.003947 ± 5	0.094809 ± 7	0.445934 ± 10	0.505038 ± 10	0.402239 ± 10
15006	0.003951 ± 5	0.094811 ± 4	0.445938 ± 7	0.505043 ± 5	0.402214 ± 7
STD*	0.003956 ± 2	0.094812 ± 2	0.445931 ± 5	0.505034 ± 3	0.402225 ± 5

Note. The number of analytical errors (2σ of the means) is given in the last digit of individual data.

energy in the region of neutron adsorption resonance, and $\sigma(E)$ is a neutron-capture cross section as a function of energy.

$\sigma_{epi} = \frac{RI}{\int_{E_c}^{E_{max}} \frac{dE}{E}}$ is given as an average cross section of the energy range between E_c and E_{max} over the thermal energy from RI divided by the integral of dE/E. Epithermal neutron-capture cross sections for individual isotopes in this study are calculated by the determination of E_{max} from the upper energy of individual resonance peaks. Calculations were made on the basis of the data of each capture cross section along with the neutron energy given from the Evaluated Nuclear Data File (ENDF/B-VII.1) compiled by the National Nuclear Data Center at Brookhaven National Laboratory.[3] The used E_{max} values (eV) are 600 for ^{149}Sm, 5000 for ^{162}Dy, 1000 for ^{163}Dy, 7500 for ^{164}Dy, 2000 for ^{167}Er, 200 for ^{168}Yb, and 2000 for ^{169}Tm. The calculated cross sections for epithermal neutron capture are listed in Table 1.

[3] https://www.nndc.bnl.gov/sigma/index.jsp

3. Results

3.1. Isotopic Compositions of Dy, Er, and Yb

The isotopic compositions of Dy, Er, and Yb of seven samples from the A-15 drill core are listed in Tables 3(a), (b), and (c), respectively. The analytical uncertainties of the individual isotopic data are 2σ of the means. Small but significant variations are found in the isotopic ratios of $^{162}Dy/^{161}Dy$, $^{164}Dy/^{161}Dy$, $^{167}Er/^{166}Er$, $^{168}Er/^{166}Er$, and $^{168}Yb/^{174}Yb$, related possibly to individual neutron-capture reactions. Among these variations, the isotopic decrements of $^{167}Er/^{166}Er$ quantitatively correspond to the increments of $^{168}Er/^{166}Er$. Figure 1(a) shows a three-isotope plot diagram for $^{167}Er/^{166}Er$ versus $^{168}Er/^{166}Er$ to identify the occurrence of the (n,γ)-type neutron-capture reaction, which are shown similarly to those for $^{149}Sm/^{152}Sm$ versus $^{150}Sm/^{152}Sm$ and for $^{157}Gd/^{160}Gd$ versus $^{158}Gd/^{160}Gd$ in previous studies (Russ et al. 1972; Hidaka et al. 2000). The data points in Figure 1(a) are plotted on the line with a slope of −1 within the analytical uncertainties, showing clear evidence for the occurrence of the neutron-capture reaction of $^{167}Er(n,\gamma)^{168}Er$.

Interpretation of the Dy isotopic variations is not simple, because multiple neutron-capture reactions of $^{162}Dy(n,\gamma)^{163}Dy$, $^{163}Dy(n,\gamma)^{164}Dy$, and $^{164}Dy(n,\gamma\beta^-)^{165}Ho$ might have occurred

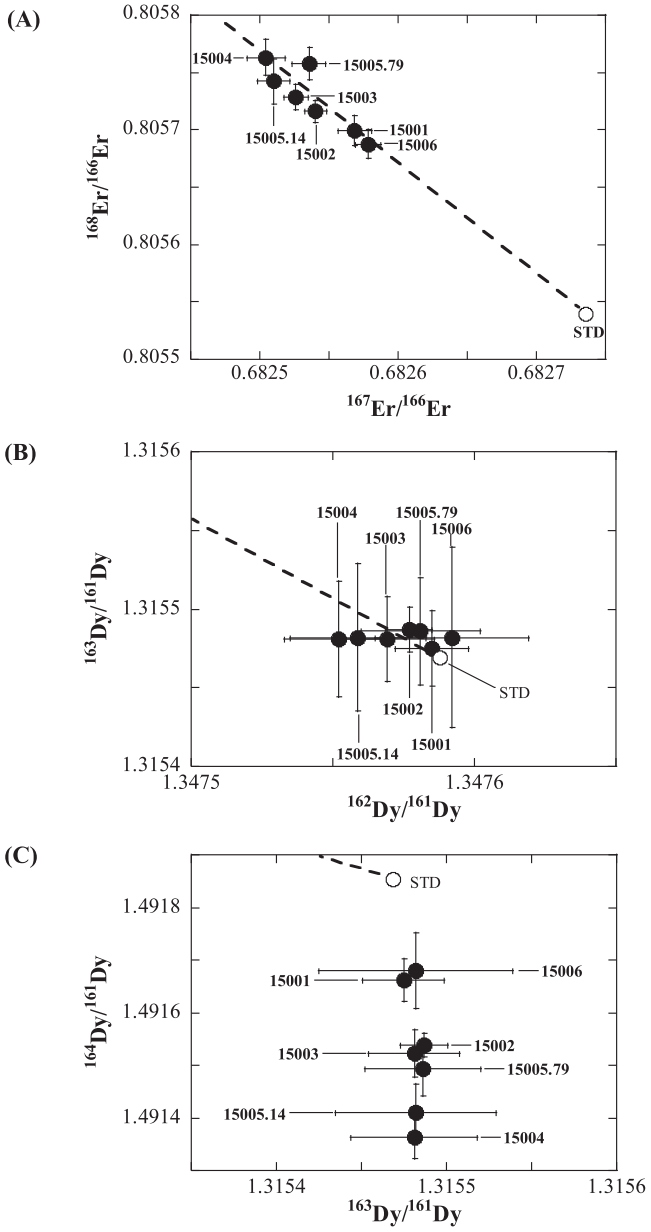

Figure 1. Three-isotope diagrams to show the correlation between (A) ^{167}Er/^{166}Er and ^{168}Er/^{166}Er, (B) ^{162}Dy/^{161}Dy and ^{163}Dy/^{161}Dy, and (C) ^{163}Dy/^{161}Dy and ^{164}Dy/^{161}Dy of the A-15 drill-core samples.

simultaneously on ^{162}Dy, ^{163}Dy, and ^{164}Dy isotopes, respectively. As a result, the data points in three-isotope plot diagrams for ^{162}Dy/^{161}Dy versus ^{163}Dy/^{161}Dy and for ^{163}Dy/^{161}Dy versus ^{164}Dy/^{161}Dy do not reveal a typical signature of the (n, γ)-type of neutron capture, as shown in Figures 1(b) and (c), respectively. The isotopic decrements of ^{162}Dy/^{161}Dy found in two of the seven samples, 15004 and 15005.14, do not correspond to the increments of ^{163}Dy/^{161}Dy. Only the trend of ^{164}Dy isotopic depletions found in all seven samples reveals that the neutron capture of ^{164}Dy is a dominant reaction rather than the other two reactions of ^{162}Dy and ^{163}Dy, which can be expected from the sizes of the individual cross sections listed in Table 2. Regarding the Yb isotopic composition, small but significant depletions of ^{168}Yb, derived probably from ^{168}Yb(n,$\gamma\beta^{+}$)^{169}Tm, can be observed in some but not all samples. Although isotopic excess of ^{170}Yb originating from ^{169}Tm(n,$\gamma\beta^{-}$)^{170}Yb is expected, it cannot be found in all samples because of less sensitivity of ^{169}Tm to both thermal and epithermal neutrons.

3.2. Depth Profiles of Dy, Er, and Yb Isotopic Variations

The neutron fluence from ^{158}Gd/^{157}Gd and ^{150}Sm/^{149}Sm isotopic shifts as a function of depth at the A-15 site was discussed by Russ et al. (1972) and Hidaka et al. (2000). Both these previous studies indicated the depth profile of the neutron fluence with an asymmetric peak at $\sim$190 g cm^{-2} from the surface. The depth profile of ^{150}Sm/^{149}Sm obtained in this study is in a good agreement with that of ^{158}Gd/^{157}Gd and ^{150}Sm/^{149}Sm reported previously (Russ et al. 1972; Hidaka et al. 2000). Although the ^{168}Er/^{167}Er isotopic ratio has a small variation relative to those of ^{150}Sm/^{149}Sm and ^{158}Gd/^{157}Gd, the depth profile of the ^{168}Er/^{167}Er isotopic variation is quite similar to those of ^{158}Gd/^{157}Gd and ^{150}Sm/^{149}Sm with an asymmetric peak at $\sim$190 g cm^{-2} (Figure 2(a)).

The depth profile of the ^{164}Dy/^{161}Dy isotopic ratio of A-15 drill-core samples is shown in Figure 2(b). As expected, the ^{164}Dy/^{161}Dy isotopic ratio decreases in a depth direction and has a minimum peak at a depth of around 200 g cm^{-2} because of the neutron-capture reaction of ^{164}Dy(n, $\gamma\beta^{-}$)^{165}Ho. As shown in Table 3(a), the isotopic depletion of ^{162}Dy/^{161}Dy was observed in two of seven samples, 15004 and 15005.14, over the analytical uncertainties, while no isotopic variations of ^{163}Dy/^{161}Dy were in all seven samples. Multiple neutron-capture reactions occur simultaneously on ^{162}Dy, ^{163}Dy, and ^{164}Dy isotopes by ^{162}Dy(n, γ)^{163}Dy, ^{163}Dy(n, γ)^{164}Dy, and ^{164}Dy(n, $\gamma\beta^{-}$)^{165}Ho, respectively. These multiple reactions on the three Dy isotopes can make the variation of intermediate isotope ^{163}Dy unclear.

Although the isotopic variations of ^{168}Yb/^{174}Yb in three of the seven samples, 15001, 15002, and 15006, were indistinguishable from the standard values within the analytical uncertainties, all of them roughly form a function of depth as shown in Figure 2(c).

4. Discussion

Our major goal is to understand isotopic evidence around the significant production of epithermal neutrons in the subsurface of the Moon. The isotopic shift from ^{167}Er to ^{168}Er in association with the neutron-capture reaction of ^{167}Er(n,γ)^{168}Er will be expected to be used for the estimation of the epithermal neutron fluences, as ^{167}Er is sensitive to epithermal neutrons because of the large RI. Since the neutron-capture reaction of ^{167}Er is an (n,γ)-type, the isotopic decrement of ^{167}Er quantitatively corresponds to the isotopic increment of ^{168}Er. The Er isotopic data set in Table 3(b) shows significant isotopic variations of depleted ^{167}Er/^{166}Er and enriched ^{168}Er/^{166}Er in all seven samples. The correlation diagram between ^{167}Er/^{166}Er and ^{168}Er/^{166}Er shown in Figure 1(a) reveals clear evidence for the occurrence of neutron capture in all seven samples of the A-15 drill core.

4.1. Estimation of Epithermal Neutron Fluences from Er Isotopic Variations

Considering that the ^{168}Er/^{167}Er isotopic shift is produced not only from thermal but also from epithermal neutron-capture reactions, the epithermal neutron fluences of the A-15 samples can be evaluated from the Er isotopic data. The evaluation of

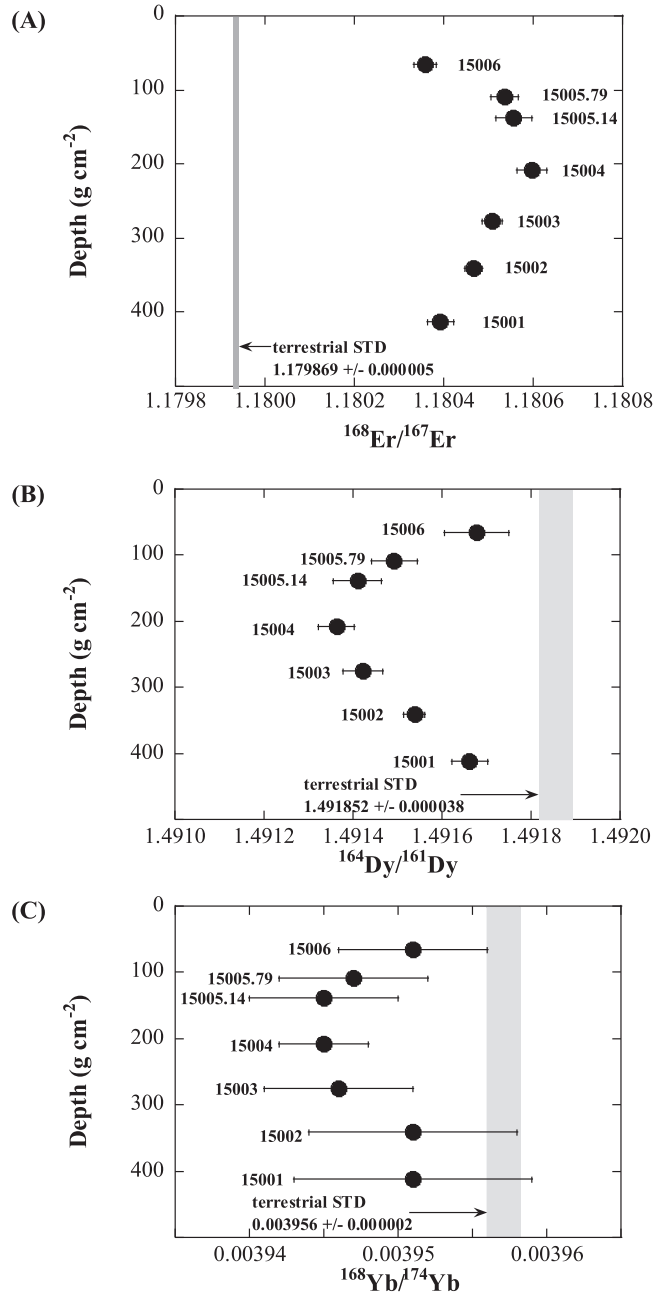

Figure 2. Depth profiles of the isotopic variations for (A) $^{168}Er/^{167}Er$, (B) $^{164}Dy/^{161}Dy$, and (C) $^{168}Yb/^{174}Yb$, possibly caused by neutron-capture reactions. The gray zone in each figure shows a terrestrial standard value without cosmic-ray irradiations.

the thermal neutron fluences of the A-15 samples is given by the Sm isotopic shifts elucidated in previous studies (Russ et al. 1972; Hidaka et al. 2000). The contribution of thermal neutron-capture reaction to the entire isotopic shift from ^{167}Er to ^{168}Er can be quantitatively estimated from the data of the thermal neutron fluence and thermal neutron-capture cross section of ^{167}Er. The excess fraction of the isotopic shifts after subtraction of the contribution of the thermal neutron-capture reaction from the entire isotopic shift provide the epithermal neutron fluences.

In general, the rate of neutron capture of each nuclide depending on the neutron-capture cross section, neutron flux, and the number of the isotope is expressed as the following equation:

$$-\frac{dN}{dt} = \sigma\phi \cdot N. \quad (1)$$

The time integration of Equation (1) is

$$N = N_0\, e^{-\sigma\phi t} = N_0\, e^{-\sigma\Psi}, \quad (2)$$

where N_0 is the initial number of isotopes before irradiation of neutrons, N is the number of isotopes remaining after time t, σ is the neutron-capture cross section, and ϕ is the neutron flux (neutrons $cm^{-2}\,s^{-1}$). The time integration of the neutron flux, ϕt, is replaced with the neutron fluence, Ψ (neutrons cm^{-2}). The numbers of isotopes, N and N_0, in Equation (2) are replaced into the isotopic ratios, R and R_0, respectively. Then, Equation (2) is rewritten as follows:

$$\sigma\Psi = \ln\left(\frac{1+R}{1+R_0}\right), \quad (3)$$

where $R_0 = {}^{168}Er/^{167}Er$ isotopic ratio without neutron-capture reactions (standard reference material), and $R = {}^{168}Er/^{167}Er$ isotopic ratio affected by neutron-capture reactions (A-15 samples). Here, $\sigma\Psi$ can be expressed simply as the summation of thermal and epithermal neutron fractions:

$$\sigma\Psi = \sigma_{th}\Psi_{th} + \sigma_{epi}\Psi_{epi}, \quad (4)$$

where σ_{th} is a thermal neutron-capture cross section, σ_{epi} is an epithermal neutron-capture cross section, Ψ_{th} is a thermal neutron fluence, and Ψ_{epi} is an epithermal neutron fluence. Since the σ_{th} of ^{149}Sm is very large, as shown in Table 1, the Sm isotopic data of A-15 samples were used only for the evaluation of the Ψ_{th} values in previous studies (Russ et al. 1972; Hidaka et al. 2000). The computed results of the neutron fluxes for several types of lunar soils showed that the Ψ_{epi} values within the lunar subsurface are more than 10 times higher than Ψ_{th} (Lawrence et al. 2006; Yamashita et al. 2008). The results suggest that Sm isotopic data are influenced by not only thermal neutrons but also epithermal neutrons, and the Ψ_{th} values should be reevaluated considering the contribution of Ψ_{epi}. In this study, Ψ_{th} and Ψ_{epi} can be determined simultaneously from Equation (4) consisting of Sm and Er isotopic data in this study. The results are listed in Table 4. The evaluated Ψ_{epi} values are in the range of (5.4–8.1) $\times$ 10^{17} n cm^{-2}, which are 11–12 times higher than Ψ_{th}. The numerical calculation for neutron production at the lunar surface suggests that the epithermal neutron flux for the A-15 soils is around 15 times higher than the thermal neutron flux (Lawrence et al. 2006), which is in good agreement with our estimation from the Er isotopic data in this study.

4.2. Estimation from Dy Isotopic Variations

Three of seven Dy stable isotopes, ^{162}Dy and ^{163}Dy having large RIs over 10^3 barns, and ^{164}Dy with a large σ_{th}, are expected to change their isotopic abundances by epithermal and thermal neutron-capture reactions, respectively. The isotopic abundances of ^{156}Dy and ^{158}Dy are too small to refer these isotopes for normalization. Although $^{164}Dy/^{162}Dy = 1.107$ was used as a normalization factor in the recent isotopic studies on Dy (Shollenberger et al. 2018), this cannot be used in this

Table 4
The Evaluation of the Thermal (Ψ_{th}) and Epithermal Neutron Fluences (Ψ_{epi}) of the A-15 Samples (Unit in $\times 10^{17}$ neutrons cm^{-2})

Sample	Estimation1[a]			Estimation2[b]		
	Ψ_{th}	Ψ_{epi}	Ψ_{epi}/Ψ_{th}	Ψ_{th}	Ψ_{epi}	Ψ_{epi}/Ψ_{th}
15001	0.48 ± 0.03	5.9 ± 0.3	12.2 ± 0.9	0.51 ± 0.81	3.2 ± 5.2	···
15002	0.57 ± 0.02	6.7 ± 0.2	11.7 ± 0.5	0.60 ± 0.85	3.2 ± 4.4	···
15003	0.63 ± 0.02	7.1 ± 0.2	11.2 ± 0.5	0.63 ± 0.32	6.7 ± 3.4	10.6 ± 7.5
15004	0.69 ± 0.03	8.1 ± 0.4	11.7 ± 0.7	0.70 ± 0.19	7.4 ± 2.0	10.6 ± 4.1
15005.14	0.65 ± 0.03	7.7 ± 0.4	11.8 ± 0.8	0.65 ± 0.30	7.4 ± 3.4	11.3 ± 7.3
15005.79	0.61 ± 0.03	7.5 ± 0.3	12.3 ± 0.8	0.62 ± 0.35	6.0 ± 3.3	9.6 ± 7.6
15006	0.51 ± 0.03	5.4 ± 0.3	10.6 ± 0.7	0.53 ± 0.53	3.2 ± 3.2	···

Notes.
[a] The estimates from $^{150}Sm/^{149}Sm$ and $^{168}Er/^{167}Er$ isotopic ratios.
[b] The estimates from $^{150}Sm/^{149}Sm$ and $^{168}Yb/^{171}Yb$ isotopic ratios.

study because of the possible variation of isotopic abundances of ^{162}Dy and ^{164}Dy by neutron-capture reactions. Considering that the isotopic abundances of ^{160}Dy and ^{161}Dy have varied less during the interaction with GCR, the $^{160}Dy/^{161}Dy$ isotopic ratio is fixed at 0.123384 and used for the normalization to make a correction for instrumental mass fractionation during the isotopic analyses.

The isotopic variations of $^{162}Dy/^{161}Dy$ and $^{163}Dy/^{161}Dy$ caused by the neutron-capture $^{162}Dy(n,\gamma)^{163}Dy$ and $^{163}Dy(n,\gamma)^{164}Dy$, respectively, are not large enough to be resolved from the standard reference values over the analytical uncertainties. As shown in Table 3(a), the isotopic ratios of $^{162}Dy/^{161}Dy$ in two of the seven samples, 15004 and 15005.14, show small depletions over the analytical uncertainties, but those in the other five samples show little variation within the uncertainties. In addition, isotopic variations of $^{163}Dy/^{161}Dy$ in all seven samples are unclear, probably because of simultaneous reactions of enrichment of ^{163}Dy by $^{162}Dy(n,\gamma)^{163}Dy$ and of depletion of ^{163}Dy by $^{163}Dy(n,\gamma)^{164}Dy$. ^{163}Dy is an intermediate product of the three neutron-capture reactions. The production rate of ^{163}Dy is expressed as follows:

$$\frac{dN_{163}}{dt} = \sigma_{162} \cdot \phi \cdot N_{162} - \sigma_{163}\phi \cdot N_{163}.$$

Considering the similarity of the size of cross sections and the number of isotopes between ^{162}Dy and ^{163}Dy, the isotopic increments of ^{163}Dy from $^{162}Dy(n,\gamma)^{163}Dy$ and the decrements by $^{163}Dy(n,\gamma)^{164}Dy$ are approximately balanced within the analytical uncertainties. This is the reason why the isotopic variations of ^{163}Dy were not detected over the analytical uncertainties in all samples, although small variations were found in the ^{162}Dy isotope for two of the seven samples.

On the other hand, significant depletions of ^{164}Dy isotopic abundances were found in all seven samples, and showed a depth dependence as presented in Figure 2. The depletions of ^{164}Dy in the A-15 samples are considered to be produced by the neutron-capture reaction $^{164}Dy(n,\gamma\beta^-)^{165}Ho$ mainly in association with thermal neutrons. Their depletion degree seems to be consistent with the evaluated thermal neutron fluences from Sm isotopic data. The quantities of ^{165}Ho produced from the neutron-captured ^{164}Dy cannot be obtained directly from the isotopic study, because ^{165}Ho is a monoisotopic element. Judging from the size difference of the neutron-capture cross section between thermal and epithermal regions as shown in Table 1, the isotopic variation of ^{164}Dy is caused dominantly by thermal neutrons. The results from the Dy isotopic data may give considerable underestimates for the epithermal fluences because of the lower sensitivity of the ^{164}Dy isotope to epithermal neutrons.

4.3. Estimation from Yb Isotopic Variations

Considering the data of the neutron-capture cross section and evaluated neutron fluences of the A-15 samples from previous studies (Russ et al. 1972; Hidaka et al. 2000), depletion of the ^{168}Yb would be expected because of the possible occurrence of the neutron-capture reactions of $^{168}Yb(n,\gamma\beta^+)^{169}Tm$. Since the neutron-capture reaction of ^{168}Yb is not an (n,γ)-type, the balance between the depletion of the parent isotope ^{168}Yb and the excess of the daughter isotope ^{169}Tm cannot be identified from the isotopic analyses of Yb alone. Additionally, the absolute amount of ^{169}Tm produced from ^{168}Yb cannot be quantitatively evaluated from the isotopic analyses, because Tm is a monoisotopic element. Small but significant depletions of ^{168}Yb isotopic abundances could be found in four of the seven samples, while those in the other three cannot be resolved from the nonirradiation standard reference value within the analytical uncertainties (see in Table 3(c)). Considering the depth dependence of neutron production rates induced by the cosmic-ray irradiation on the surface of the Moon (Russ et al. 1971; Hidaka et al. 2000), the depth dependence on the isotopic variations of ^{168}Yb is the only way to judge the possible occurrence of neutron-capture reactions.

Since the isotopic abundance of ^{168}Yb is originally very low, the isotopic data in all seven samples hold relatively large analytical uncertainties. The isotopic depletions of ^{168}Yb, however, have a depth dependence as shown in Figure 2(c). As for the similar case of Er isotopic variations, shown in Table 4, the epithermal neutron fluences of (6.0–7.4) $\times 10^{17}$ n cm^{-2} were evaluated from the ^{168}Yb isotopic variations in four of seven samples. Considering the analytical uncertainties of the Yb isotopic data, these estimates are consistent with those given by the Er isotopic data. Although high-precision isotopic analysis is required to detect the isotopic depletions of ^{168}Yb because of its minor isotopic abundance, it has a great advantage when estimating the fluences of epithermal neutrons because of the high sensitivity of ^{168}Yb to epithermal neutrons.

5. Conclusions

As a result of systematic REE isotopic analyses, significant variations of ^{164}Dy, ^{167}Er, ^{168}Er, and ^{168}Yb isotopic abundances caused by neutron-capture reactions induced by GCR

irradiation were newly found together with ^{149}Sm, ^{150}Sm, ^{157}Gd, and ^{158}Gd in a series of A-15 drill-core samples. Since thermal neutron capture is the dominant reaction for the ^{164}Dy isotope, the use of Dy isotopic data did not allow the epithermal neutron fluences to be well estimated. In contrast, ^{168}Yb, ^{167}Er, and ^{168}Er isotopic data can be good indices for the estimation of epithermal neutron fluence. In particular, the isotopic shift of ^{168}Er/^{167}Er, showing a clear function of the depth in the core, provided an estimation of (5.4–8.1) $\times$ 10^{17} n cm^{-2} for epithermal neutron fluences. Although the Sm isotopic data of A-15 samples were used only for the estimation of thermal neutron fluences in previous studies, they were also influenced by epithermal neutrons. As a result of the reevaluation, (4.8–6.9) $\times$ 10^{16} n cm^{-2} for epithermal neutron fluences were given by the combination of the ^{150}Sm/^{149}Sm and ^{168}Er/^{167}Er isotopic data set. This is the first report to evaluate the thermal and epithermal neutron fluences from the isotopic variations of the lunar materials.

ORCID iDs

Hiroshi Hidaka https://orcid.org/0000-0001-7239-4086
Shigekazu Yoneda https://orcid.org/0000-0003-2306-4261

References

Albalat, E., Blichert-Toft, J., Telouk, P., & Albarède, F. 2015, E&PSL, 429, 147
Curtis, D. B., & Wasserburg, G. J. 1975, Moon, 13, 185
Feldman, W. C., Barraclough, B. L., Maurice, S., et al. 1998a, Sci, 281, 1489
Feldman, W. C., Lawrence, D. J., Elphic, R. C., et al. 2000, JGR, 105, 20347
Feldman, W. C., Maurice, S., Binder, A. B., et al. 1998b, Sci, 281, 1496
Hidaka, H., Ebihara, M., & Yoneda, S. 2000, M&PS, 35, 581
Hidaka, H., Sakuma, K., Nishiizumi, K., & Yoneda, S. 2017, AJ, 153, 274
Hidaka, H., & Yoneda, S. 2007, GeCoA, 71, 1074
Hidaka, H., Yoneda, S., & Nishiizumi, K. 2009, E&PSL, 288, 564
Kruijer, T. S., Sprung, P., Kleine, T., Leya, I., & Wieler, R. 2013, M&PS, 48, 2597
Lawrence, D. J., Feldman, W. C., Elphic, R. C., et al. 2006, JGR, 111, E08001
Leya, I., & Masarik, J. 2013, M&PS, 48, 665
Leya, I., Wieler, R., & Halliday, A. N. 2003, GeCoA, 67, 529
Lingenfelter, R. E., Canfield, E. H., & Hampel, V. E. 1972, E&PSL, 16, 355
Lingenfelter, R. E., Canfield, E. H., & Hess, W. N. 1961, JGR, 66, 2665
Mizutani, Y., Hidaka, H., & Yoneda, S. 2020, GeocJ, in press
Nishiizumi, K., Elmore, D., Ma, X. Z., & Arnold, J. R. 1984a, E&PSL, 70, 157
Nishiizumi, K., Fink, D., Klein, J., et al. 1997, E&PSL, 148, 545
Nishiizumi, K., Klein, J., Middleton, R., & Arnold, J. R. 1984b, E&PSL, 70, 164
Russ, G. P., Burnett, D. S., Lingenfelter, R. E., & Wasserburg, G. J. 1971, E&PSL, 13, 53
Russ, G. P., III, Burnett, D. S., & Wasserburg, G. J. 1972, E&PSL, 15, 172
Sands, D. G., De Laeter, J. R., & Rosman, K. J. R. 2001, E&PSL, 186, 335
Shollenberger, Q. R., Render, J., & Brennecka, G. A. 2018, E&PSL, 495, 12
Spergel, M. S., Reedy, R. C., Lazareth, O. W., et al. 1986, JGR, 91, D483
Yamashita, N., Hasebe, N., Miyachi, T., et al. 2008, EP&S, 60, 313